TD-DFT Investigation of the UV Spectra of Pyranone Derivatives

Julien Preat,* Denis Jacquemin, Valérie Wathelet, Jean-Marie André, and Eric A. Perpète

Laboratoire de Chimie Théorique Appliquée, Facultés Universitaires Notre-Dame de la Paix, 61 Rue de Bruxelles, 5000 Namur, Belgium

Received: February 28, 2006; In Final Form: May 9, 2006

The UV absorption spectra of more than 80 substituted coumarins and chromones have been investigated with the PCM-TD-DFT theoretical scheme using three hybrid functionals (O3LYP, B3LYP, and PBE0) and taking into account methanol or ethanol solvation effects. For most of the studied derivatives, there are at least two allowed excited states presenting a strong oscillator strength in the UV region. The first allowed excitation is associated to a HOMO−LUMO transition whereas the second corresponds to a transition from the HOMO-1 to the LUMO. Both involve a charge transfer from the benzenic cycle to the pyranone moiety. Statistically treating the PBE0 results allows a prediction of the λ_{max} with small standard deviations: in methanol, 6 nm (0.07 eV) for the first excitation ($\lambda_{max}^{(1)}$) and 5 nm (0.08 eV) for the second one ($\lambda_{max}^{(2)}$), whereas in ethanol 6 nm (0.08 eV) for $\lambda_{max}^{(1)}$ and 6 nm (0.13 eV) for $\lambda_{max}^{(2)}$.

Introduction

The compounds of the pyranone class, especially those based on coumarin or on chromone cores, give rise to one of the most extensively investigated and commercially used group of organic materials. Pyranone derivatives are built from two fused aromatic cycles (Figure 1), which can easily be functionalized by several side groups. These compounds owe their success to their tailorable properties combined to a high stability. For instance, the coumarin derivatives are of considerable biological and medical interest because they show anticoagulant activity effects, though remaining weakly toxic.[1] In physicochemical applications, their light emission abilities make them the main fluorescent dyes used in paints and inks. Indeed, these dyes, often absorbing in the UV region, emit blue-green light and are known to be efficient fluorescent brighteners.[2] In 1929, Krais treated rayon and flax with an extract composed of husks of horse chestnut to make them waterproof. This extract contained esculin, a fluorescent glucoside now known as 6,7-dihydroxy-coumarin. The first industrial optical brightener was methyl-umbelliferone (4-Me,7-OH coumarin), which is easily obtained from resorcinol (benzene 1,3-diol) and 3-oxobutanoate. In 1999, the world production of fluorescent brighteners amounted to 40 000 tons of active substances.[3] Nowadays, some special fluorescent brighteners are also applied in laser-dye technology, and there is a huge interest in the design of new compounds able to emit in the yellow-red region of the visible spectrum.

As a first step toward the fluorescent spectra of these derivatives, one needs to set up an efficient theoretical scheme able to provide absorption energies with a high accuracy. In this scope, we seek the rationalization and the evaluation of the λ_{max} of absorption for a series of pyranone dyes. The molecular modelization techniques now offer a competitive alternative for the interpretation of experimental data arising from industrial interest and applications. Though sometimes useful for a qualitative insight on experimental features, semiempirical calculations do not qualify to reproduce the high accuracy obtained with more elaborated ab initio approaches. The reported studies of the coumarin electronic structure are usually combined with experimental methods: UV photoelectron spectra (UPS) or UV/VIS spectroscopy.[4,5] The related theoretical investigations have been performed at the Pariser−Parr−Pople (PPP), CNDO/S3, or AM1 levels of approximation with which only pretty average results where produced. For instance, Kachovski et al. obtained PPP and AM1 λ_{max} in puzzling agreement with spectroscopic data in ethanol, although solvent effects were not explicitely included in their model.[6] In this contribution, we use the ab initio time-dependent density functional theory (TD-DFT), which is often found to be a robust and accurate method for evaluating the low-lying excited states of conjugated molecules and has been thoroughly applied to solve chemical and physical problems.[7−14] Cave et al. studied the absorption and emission spectra of six coumarins (coumarin 102, 120, 151, 152, 153, and 343) by using various ab initio frameworks (DFT, CIS, ...) and the 6-311G(d,p) basis set.[15,16] These studies have been carried out for selected derivatives only and are therefore not completely compatible with our approach that we wish to be as general as possible. Up to now, no general methodology able to provide reliable predictions of UV spectra of coumarin derivatives in solvent-phase has, to our knowledge, been built up. In this paper, our aim is to set up such a general theoretical procedure, and we strive after the 10−15 nm accuracy that is required for the design of new coumarins and chromones. To hit this target, we use the PCM-TD-DFT/6-311+G(2d,2p)//PCM-B3LYP/6-311G(2d,2p) computational scheme that leads to converged λ_{max} as shown by our initial methodological investigation.[11]

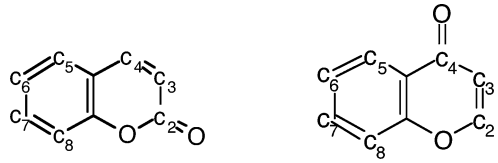

Figure 1. Sketch of coumarin (left) and chromone (right) with numbering of the substitution positions.

* Corresponding author. Tel: +32(0)81 724568. Fax: +32(0)81 724567. E-mail: julien.preat@fundp.ac.be.

10.1021/jp061260r CCC: $33.50
Published on Web 06/15/2006

Methodology

All calculations have been performed with the Gaussian 03[17] package, following a two-step procedure: (i) the optimization of the ground-state geometry with DFT and (ii) the determination of the vertical electronic transition energies by means of TD-DFT.[18]

The geometry optimizations have been performed with a *tight* threshold that corresponds to root mean square (rms) residual forces smaller than 10^{-5} au for the optimal geometry. After the minimization process, we check the vibrational spectrum to ensure that no imaginary frequency is present. The vibrational frequencies have been evaluated by the analytical determination of the Hessian matrix, consistently using the same level of theory as in the previous step. However, one should keep in mind that, for coumarin derivatives presenting large side groups, local minima might show up and that the absence of negative eigenvalues does not straightforwardly imply the global minimum.

DFT orbitals are obtained by solving the Kohn−Sham equation, involving exchange and correlation (XC) terms. Numerous XC functionals have been developed, and an adequate choice is crucial to obtain reliable results. The functionals used in most studies can be classified in (at least) three groups. In a first group, one finds the local density approximation (LDA) functionals. In this scheme, the potential due to a spherical and uniform distribution of the charge density is allocated to each electron. Consequently, this approximation is often inappropriate for studying the excitation spectra of conjugated organic molecules. In a second group, one finds the gradient corrected functionals (GGA for generalized gradient approximation), for example, BLYP [Becke's exchange[19] and Lee−Yang−Parr (LYP)[20] correlation] and PBE[21] (Perdew−Burke−Erzenrhof). Here, the exchange-correlation potential is a function of both the density and its gradient. More elaborated functionals such as the van Voohris and Scuseria τ-shaped VSXC[22] of *meta*-GGA type, include the density Laplacian or other high-order term in the XC potential. Compared to LDA, GGA and *meta*-GGA functionals provide superior results, but they are still unable to deliver correct values for most molecular properties (geometries, UV/VIS spectra) of organic dyes. In a third group, one finds the hybrid functionals that are currently in the mood for computational chemistry and include a fraction of Hartree−Fock (HF) exchange. In the present work, three hybrids have been used: O3LYP,[23] B3LYP,[24] and PBE0,[25,26] including HF exchange percentages of 11.61%, 20%, and 25%, respectively. The two first hybrids are representative of the so-called ACM3 approach and are written as

$$E^{\mathrm{XC}} = E^{\mathrm{LDA-SC}} + \beta_1(E^{\mathrm{HF}} - E^{\mathrm{LDA-HF}}) + \beta_2 \Delta E^{\mathrm{GGA-X}} + \beta_3 \Delta E^{\mathrm{GGA-C}} \quad (1)$$

where the GGA corrections on the exchange and correlation energies explicitly appear. The β_i are often optimized by a least-squares fit on experimental data of gas-phase molecules (such as atomization heats, ionization potentials, electroaffinities, ...). In O3LYP ($\beta_1 = 0.1161$, $\beta_2 = 0.9262$, and $\beta_3 = 0.8133$), the GGA correction on the exchange is provided by OPTX[27] whereas the correction on the correlation involves the LYP functional. In B3LYP ($\beta_1 = 0.20$, $\beta_2 = 0.72$, and $\beta_3 = 0.83$), one uses Becke's exchange and LYP correlation. PBE0 ($\beta_1 = 0.25$) is built on the ACM1 model:

$$E^{\mathrm{XC}} = \beta_1 E^{\mathrm{HF}} + (1 - \beta_1) E^{\mathrm{GGA-X}} + E^{\mathrm{GGA-C}} \quad (2)$$

where β_1 is fixed on the basis of theoretical considerations. We have selected the 6-311G(2d,2p) basis set (BS) with the B3LYP functional for the ground-state optimizations and 6-311G+(2d,-2p) for the TD-DFT calculations. These BS have been shown to return converged $\lambda_{\max}$ for a series of coumarins,[11] smaller BS yielding too small $\lambda_{\max}$ (in nm).

From a pratical point of view, the coumarins are often used in solution. Formally, the solvent effects can be split into two components: (i) a perturbation of the UV spectrum (*direct* effect) and (ii) a modification of the ground-state geometry (*indirect* effect). In coumarins, the direct effects are huge [$\sim$12 nm bathoshift in EtOH] and have to be taken into account. Moreover, the change in the ground-state geometry due to solvation has small but systematic [$\sim$2 nm bathoshift in EtOH] impact on $\lambda_{\max}$ and must also be considered for obtaining the required accuracy. Consequently, the polarizable continuum model (PCM)[28,29] is used for evaluating the (bulk) solvent effects. In PCM, one divides the problem into a solute part (the dye) and a solvent part (we have chosen methanol and ethanol, as in the experiment) represented as a structureless material, characterized by its dielectric constant as well as other parameters. PCM is able to obtain a valid approximation of solvent effects as long as there is no specific interaction between the solute and the solvent. We have selected the so-called nonequilibrium PCM solutions, and we refer the reader to ref 12 for extensive details about this procedure.

To reach the best agreement between theory and experiment, the results from different approaches are treated by means of a simple linear regression (SLR) scheme[30−32] that analyzes the relationship between one dependent variable (the experimental value) and one independent variable (theoretical values or properties). To test the significance of a regression, the total sum of squares (TSS) is split into two components: the model sum of squares (MSS) and the residual sum of squares (RSS). If the mathematical model passes through all the original data points, the MSS is equal to the TSS, the RSS is zero, and the relationship between the dependent and the independent variable is meaningful. The accuracy associated to the regression is measured with the mean average error (MAE), and the level of the prediction accuracy is provided by the standard deviation of the residual (SDR), whereas the prediction reliability is given by the adjusted determination coefficient (adjusted R^2). The weaker the SDR, the more accurate the predictive model. In addition, the higher the adjusted R^2, the more reliable are the predictions.

Results and Discussion

UV Spectra Evaluation. The theoretical $\lambda_{\max}$ reported in the following correspond to the first singlet excited states with dipole-allowed transitions (i.e., nonzero oscillator strength f) from the ground state. Although we express the excitation energies in nanometers because this unit is often used by colorists, electronvolts are used for the statistical treatment as they are more "physical units". For most of the studied derivatives, there are two allowed states close in energy in the UV/VIS region, characterized by a large transition probability.[33−37] The first absorption band [$\lambda_{\max}^{(1)}$] is typically of medium intensity and is observed in the vicinity of 290 nm (for chromone) and 330 nm (for coumarin). $\lambda_{\max}^{(1)}$ is associated to an excitation from the highest occupied molecular orbital (HOMO) to the lowest unoccupied molecular orbital (LUMO). The second absorption band [$\lambda_{\max}^{(2)}$] is of comparatively higher intensity and involves an excitation from the HOMO-1 to the LUMO. It is observed in the 200 nm (for chromone) and 300 nm region (for

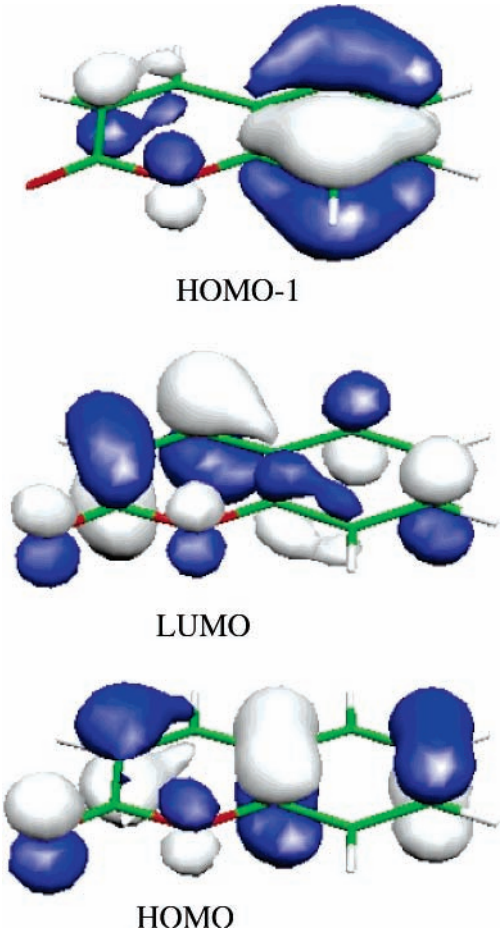

Figure 2. Representation of the coumarin HOMO-1, HOMO, and LUMO. They have been obtained at the PCM(EtOH)-B3LYP/6-311G+(2d,2p)//PCM(EtOH)-B3LYP/6-311G(2d,2p) level. For coumarin, the first excitation process involves a HOMO → LUMO transition whereas the second excitation is a HOMO-1 → LUMO transition.

coumarin) and is due to the benzenoid absorption. As can be seen on Figure 2, the excitation processes in coumarin (and chromone derviatives) involve typical $\pi \rightarrow \pi^*$ transitions and are related to a charge transfer from the benzenic cycle to the pyranone moiety, but with a larger redistribution of the charges for $\lambda_{max}^{(2)}$.

The results of the theoretical evaluations are compared with experimental measurements in Tables 1 (EtOH) and 2 (MeOH). Since $\lambda_{max}^{(1)}$ and $\lambda_{max}^{(2)}$ are not localized in the same region of the electromagnetic spectrum and are related to different molecular orbitals, we treat them distinctly. The two solvents have also to be considered separately as potential specific solute−solvent interactions are not included in the PCM model. In general TD-DFT excitation energies are within a 0.4 eV deviation from experiment.[38] For the λ_{max} of organic dyes the average errors are often smaller than this upper limit. For instance, Guillaumont and Nakamura calculated the maximum absorption wavelength of several organic dyes (indigo, azobenzene, phenylamine, hydrazone, anthraquinone, etc.) with an average deviation close to 0.20 eV.[10] For coumarins Cave et al. have estimated the C102, C152, C153, and C343 vertical energies of maximal absorption with a precission varying from 0.10 to 0.43 eV,[16] whereas in an earlier contribution the same authors provided a nice accuracy (±0.08 eV) for the C151 UV spectrum in several solvents.[15] Table 3 provides the MAE deduced from the present TD-DFT calculations. Our MAE on the whole set of λ_{max} is of the same order (between 0.10 and 0.30 eV) as these previous TD-DFT

TABLE 1: $\lambda_{max}^{(2)} - \lambda_{max}^{(1)}$ (in nm) Provided by TD-O3LYP, TD-B3LYP, TD-PBE0/6-311G+(2d,2p), and SLR Method in Ethanol[a]

	λ_{max}						
compounds	O3LYP	B3LYP	PBE0	eq 4-$\lambda_{max}^{(2)}$	eq 3-$\lambda_{max}^{(1)}$	exp	ref
coumarin	287−310	280−301	272−294	275	312	274−311	35
3-Me	290−305	281−298	273−291	276	309	275−308	35
4-Me	284−307	276−298	269−291	272	309	271−307	35
5-Me	301−321	295−309	288−300	291	317	275−315	34
6-Me	288−324	282−313	274−306	277	322	278−320	34
7-Me	294−311	285−303	276−297	279	314	283−313	34
8-Me	294−319	288−307	280−299	283	316	281−310	34
3,4-diMe	289−307	280−300	272−294	275	312	273−308	35
4,6-diMe	285−320	278−310	270−302	273	318	273−318	35
4,7-diMe	290−308	280−301	272−294	275	312	278−314	35
4,8-diMe	291−315	284−304	276−296	279	313	277−311	35
3-OH	240−314	232−308	225−301	228	318	230−311	34
4-OH	276−297	269−291	262−284	265	303	268−303	34
5-OH	247−299	239−294	233−288	235	305	250−298	34
6-OH	286−363	280−346	273−336	276	348	280−345	34
7-OH	254−321	247−313	240−306	243	322	240−325	36
8-OH	263−299	250−293	246−286	249	304	253−292	34
7,6-diOH	355	340	331		343	348	34
4-Me,5-OH	251−294	243−289	236−283	239	302	250−294	36
4-Me,6-OH	250−284	242−277	235−266	238	287	227−275	36
4-Me,7-NEt_2	285−380	248−361	244−350	247	360	243−375	34
6-Me,4-OH	307	300	293		311	314	34
3,6-diCl, 4-MeO	294−319	283−308	276−300	279	317	280−320	34
7-Cl	310	303	296		313	313	34
4-Br	291−317	284−308	277−300	280	317	277−318	34
4-MeO, 3-Me	287−303	278−296	270−289	273	307	272−310	34
4-MeO,7-OH,5-Me	249−301	240−293	233−286	235	305	225−290	34
4,6-diMeO	276−340	269−326	262−316	265	331	270−327	34
5-MeO	301	296	290		308	298	34
5-MeO, 7-OH	254−344	246−330	240−320	243	334	247−330	34
5,7-diMeO	254−317	246−304	239−295	242	312	245−325	34
6,7,8-triMeO	259−359	238−346	229−334	232	346	228−343	34
7-MeO, 8-OH	314	305	298		315	325	34
7-MeO	255−324	246−315	240−308	243	324	242−325	34
7-MeO,4-OH,5-Me	255−307	246−298	240−291	243	309	242−309	34
7-MeO, 6-OH	262−358	252−343	246−333	249	345	257−351	34
4-NMe_2	310	301	294		312	306	34
chromone	292	283	276		296	298	35
2-Me	260−290	254−282	222−275	225	295	225−295	35
2,3-diMe	264−298	258−288	227−281	229	300	225−299	35
2,6-diMe	264−299	257−290	226−283	228	302	225−303	35
2,7-diMe	270−288	263−280	223−273	225	293	225−294	35
2,8-diMe	265−298	240−288	235−280	238	299	225−299	35
3-Me	262−298	256−289	223−281	225	300	225−304	35
5-OH,2-Me	242−343	229−326	229−316	232	331	226−326	36
6-OH,2-Me	245−331	238−318	232−309	234	324	226−326	36
7-OH,2-Me	243−293	235−282	220−274	223	294	226−302	36

[a] All geometries are obtained at the B3LYP/6-311G(2d,2p) level. During the calculations, bulk solvent effects are modelized by the PCM model.

investigations. From the results listed in Table 3, it is not obvious to choose among O3LYP, B3LYP, or PBE0 on the only basis of the agreement with experimental λ_{max}. Indeed, using the MAE criterium, O3LYP appears to be the more accurate hybrid for $\lambda_{max}^{(1)}$ evaluation whereas PBE0 and B3LYP would be functionals of choice for $\lambda_{max}^{(2)}$ calculations. Actually, one is often interested in auxochromic shifts not in absolute λ_{max}. The fitted-parameter-free PBE0 yields the best agreement between theoretical and experimental shifts for the substituted pyranone (the MAE on the whole ethanol set is only of 0.07 eV for PBE0 as compared to 0.10 and 0.12 eV for B3LYP and O3LYP, respectively). Figure 3 depicts the nice correlation between PCM(EtOH)-TD-PBE0 and the experimental auxochromic

TABLE 2: $\lambda^{(2)}_{max} - \lambda^{(1)}_{max}$ (in nm) Provided by TD-O3LYP, TD-B3LYP, TD-PBE0/6-311G+(2d,2p), and SLR Method for Substituted Coumarins in Methanol[a]

	λ_{max}						
compounds	O3LYP	B3LYP	PBE0	eq 6-$\lambda^{(2)}_{max}$	eq 5-$\lambda^{(1)}_{max}$	exp	ref
3,4,6-triMe	287−315	279−306	271−299	279	316	275−318	33
3,4,7-triMe	292−311	282−304	273−298	281	315	281−313	33
4-OH	276−297	269−291	262−284	272	303	268−302	33
4,5-diOH	289	283	277		297	292	33
4,6-diOH	281−339	273−327	267−319	276	333	276−320	33
4-Me,5-OH	251−294	243−289	236−283	250	302	250−294	33
4-Me,5,7-diOH	308−332	298−318	289−309	294	324	294−320	34
4-Me 6-OH	284−357	276−341	270−331	278	343	274−342	33
4-Me,6,7-diOH	299−351	288−337	279−328	286	340	294−345	33
4-Me,7-OH	251−319	244−310	238−303	252	319	252−322	33
5-Me,7-OH	327	319	312		327	328	34
8-Me,7-OH	256−326	248−315	242−308	255	323	258−327	34
4-MeO,7-Me	276−294	268−288	261−281	271	300	267−303	34
4-MeO,8-Me	279−298	272−290	265−283	274	302	268−306	33
4,6-diMeO	276−340	269−326	262−316	272	330	280−326	33
4,7-diMeO	280−305	271−296	263−289	272	307	280−305	34
4,7,8-triMeO	296	288	282		301	304	33
5-MeO,4-OH	291	284	278		298	294	34
7-MeO,8-Me	252−330	248−318	240−310	254	345	256−323	34
6-MeO,7-OH	301−332	247−322	242−314	255	325	252−344	34
6-MeO,4-Me	284−361	277−343	270−333	278	345	273−340	34
7-MeO,4-Me	252−306	241−299	234−292	249	310	249−321	34

[a] All geometries are obtained at the B3LYP/6-311G(2d,2p) level. During the calculations, bulk solvent effects are modelized through the PCM model.

TABLE 3: MAE (in nm and eV) Related to TD-DFT Calculations in both Ethanol and Methanol

	EtOH				MeOH			
	$\lambda^{(2)}_{max}$		$\lambda^{(1)}_{max}$		$\lambda^{(2)}_{max}$		$\lambda^{(1)}_{max}$	
	nm	eV	nm	eV	nm	eV	nm	eV
O3LYP	18	0.32	6	0.07	9	0.14	8	0.09
B3LYP	10	0.19	9	0.12	6	0.10	10	0.13
PBE0	5	0.10	17	0.23	10	0.19	16	0.22
SLR−PBE0	4	0.09	4	0.05	3	0.06	5	0.06

shifts. This suggests that the theory/experiment discrepancies found with PBE0 are related to systematic and quasi-constant errors for coumarin and chromone dyes. Indeed, the sign (batho/hypso) of the shift is almost always correctly predicted: only 7 shifts (9%) present errors exceeding 10 nm, and no discrepancy larger than 15 nm is observed. Additionnally (Table 1), PBE0 efficiently simulates the differences between position isomers.

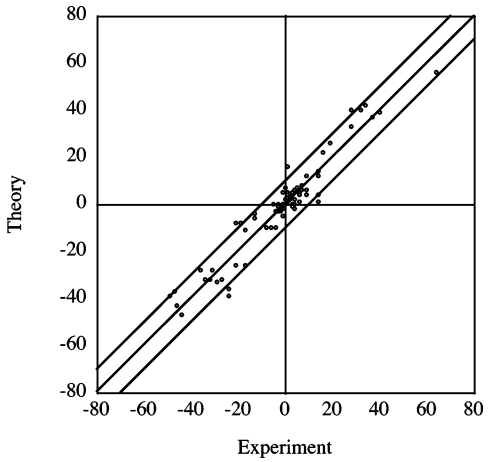

Figure 3. Comparison between experimental (EtOH) and PBE0 auxochromic shifts (in nm) for substitued forms of pyranone dye. The central line indicates a perfect match whereas the two side lines are borders for ±10 nm discrepancies.

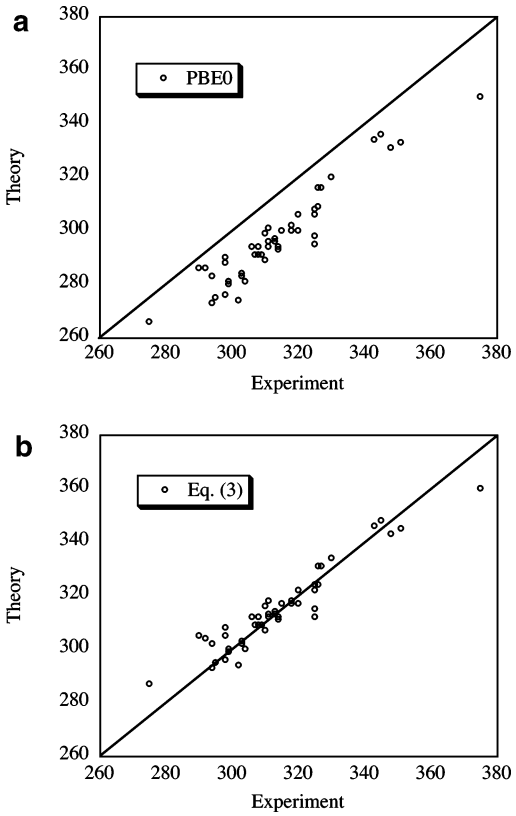

Figure 4. Comparison of experimental and theoretical $\lambda^{(1)}_{max}$ of absorption for the set of derivatives of Table 1.

For instance, the $\lambda^{(1)}_{max-EtOH}$ for 6-OH and 5-OH, differ by 47 nm in experiment, and theory provides the same value (48 nm). The $\lambda^{(1)}_{max-EtOH}$ of 4-Me,5-OH and 4-Me,6-OH are separated by 19 nm in experiment, nicely reproduced by the 15 nm theoretical difference.

From a more general point of view, the major errors between theory and experiment originates from (i) the temperature effects, which are only partly included in our solvation model; (ii) the vibrational effects that are not taken into account; and (iii) more essentially, the fact that PCM does not explicitly take into account H-bonds. Nevertheless, for the latter, dealing specific interactions requires the determination of, at least, the first of the coordination spheres embedding each compounds. It would require a huge computational efforts and would ruin our approach that we want as general as possible. The statistical treatment partly helps to correct these discrepancies.

To improve the predictive abilities of our model, a SLR treatment of TD-DFT results has been performed. It turns out that PBE0 is the most reliable hybrid: it presents the highest adjusted R^2 (0.8910 as an average over all λ_{max}). On the other hand, O3LYP is the less reliable hybrid with a 0.7481 adjusted R^2, whereas B3LYP provides an intermediate correlation coefficient. The calibration of the PBE0 λ_{max} leads to a set of four equations in such a way that the experimental values (in nm) are optimaly reproduced in both solvents. These equations allow to overcome the initial systematic λ_{max} underestimation of the TD-PBE0 calculations. For the ethanol series, the effects of this correction are shown in Figures 4 and 5. The first equation

$$\lambda^{(1)-Exp.}_{max-EtOH} = 57.475 + 0.864\,\lambda^{(1)-PBE0}_{max-EtOH} \qquad (3)$$

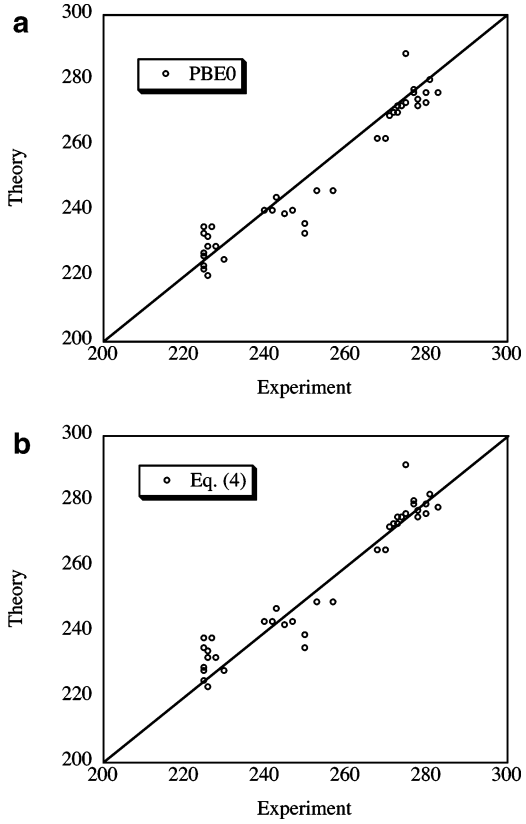

Figure 5. Comparison of experimental and theoretical $\lambda_{max}^{(2)}$ of absorption for the set of derivatives of Table 1.

provides a R^2 of 0.8902 (adjusted R^2 of 0.8878). The related MAE is limited to 4 nm (or 0.05 eV for the corresponding eV equation). Compared to the 17 nm (0.23 eV) non-fitted MAE (Table 3), eq 3 is obviously much more accurate. The SDR, which measures the magnitude of the accuracy for the design of new dyes is of 6 nm (i.e., $\lambda_{max-EtOH}^{(1)-Exp.} = \lambda_{max}^{eq3} \pm 6$ nm ($\pm$ 0.08 eV). For the second peak in ethanol, eq 4 has a high adjusted R^2 (0.9143) provides a MAE limited to 4 nm or 0.09 eV and allows a prediction with a $\pm$ 6 nm ($\pm$ 0.13 eV) error:

$$\lambda_{max-EtOH}^{(2)-Exp.} = 1.379 + 1.005\lambda_{max-EtOH}^{(2)-PBE0} \quad (4)$$

In methanol,

$$\lambda_{max-MeOH}^{(1)-Exp.} = 62.557 + 0.847\lambda_{max-MeOH}^{(1)-PBE0} \quad (5)$$

$$\lambda_{max-MeOH}^{(2)-Exp.} = 57.299 + 0.818\lambda_{max-MeOH}^{(2)-PBE0} \quad (6)$$

deliver adjusted R^2 of 0.8531 and 0.8912 with MAE values of 5 and 6 nm (or 0.06 and 0.04 eV) for $\lambda_{max}^{(1)}$ and $\lambda_{max}^{(2)}$, respectively. This is at least 3 orders of magnitude more accurate than non-fitted values. The accuracy on the prediction (SDR) is 6 nm (0.07 eV) for $\lambda_{max}^{(1)}$ and 5 nm (0.08 eV) for $\lambda_{max}^{(2)}$. Similar statistical post-treatments have been peformed on B3LYP and O3LYP results, and as expected, it turns out that they remain less accurate than PBE0. Indeed, the MAE for all the λ_{max} are of 7 nm (0.10 eV) for O3LYP and 5 nm (0.09 eV) for B3LYP at least 0.03 eV higher than their PBE0 counterpart, backing up our choice for PBE0 in the pyranone study. SLR post-treatment authorizes a more accurate evaluation of excitation energies for most position isomers and can also resolve difficult cases (methoxy-derivatives), while limiting the largest theory/experiment discrepancies to relatively small figures (13 nm for 5,7-diMeO $\lambda_{max-EtOH}^{(1)}$ and 10 nm for 7-MeO,8-OH $\lambda_{max-EtOH}^{(1)}$) in cases where TD-PBE0 gives larger errors (30 nm for 5,7-diMeO and 27 nm for 7-MeO,8-OH). For the amino derivatives, the correction of theoretical results is weaker, that is, the theory/experiment discrepancies remain substantial: 15 nm for 4-Me,7-NEt_2 $\lambda_{max-EtOH}^{(1)}$ and 12 nm for C440 $\lambda_{max-EtOH}^{(1)}$, as shown in Tables 1 and 4. For this type of compounds, the *free* rotation around the bond between the amine and the coumarin core might be activated in solution. Indeed for 4-CF_3,7-NH_2-coumarin (also known as C151), Cave et al.[15] obtained a structural local minimum featuring a ring-N−H angle of 60° (its value is 20° at the global minimum) for which the calculated ground-state

TABLE 4: Comparison between the Experimental (EtOH) and Theoretical $\lambda_{max}^{(2)} - \lambda_{max}^{(1)}$ of Coumarin Derivatives[a]

compounds	O3LYP	B3LYP	PBE0	eq 4-$\lambda_{max}^{(2)}$	eq 3-$\lambda_{max}^{(1)}$	exp (EtOH)	ref
7-Me,6-NO_2	296−366	287−346	280−329	283	342	264−316	33
7,8-diOH	355	335	324		337	335	34
7-Me,4-OH	280−300	2723−293	265−287	268	305	245−304	34
7-NH_2,4-Me (C440)	351	338	329		342	354	37
C540A	444	420	406		408	422	37
azomethine-A	329−370	288−352	289−348	292	358	278−344	6
azomethine-B	304−354	290−342	281−332	284	344	293−321	6
azomethine-C	303−385	293−368	286−358	289	369	278−365	6
azomethine-D	303−341	290−331	282−321	285	335	274−328	6
azomethine-E	303−361	293−348	287−339	290	350	287−339	6
azomethine-F	375−527	357−484	342−454	345	450	279−385	6
azomethine-G	410−402	374−396	355−384	358	389	269−356	6

[a] All values are in nm.

TABLE 5: Comparison between the Experimental (MeOH) and Theoretical $\lambda_{max}^{(2)} - \lambda_{max}^{(1)}$ of Coumarin Derivatives[a]

compounds	O3LYP	B3LYP	PBE0	eq 6-$\lambda_{max}^{(2)}$	eq 5-$\lambda_{max}^{(1)}$	exp (MeOH)	ref
4,7-diOH	304	298	291		309	304	34
7,5-diOH	254−319	247−309	240−300	254	317	263−329	34
3,4-diMe,7-OH	321	312	304		320	322	34
7-MeO,5-Me	252−333	245−323	239−314	253	328	256−327	34
4,7-diMeO,5-Me	305	296	289		307	306	34
5,7-diMeO,4-Me	256−340	247−325	241−316	255	330	252−320	34

[a] All values are in nm.

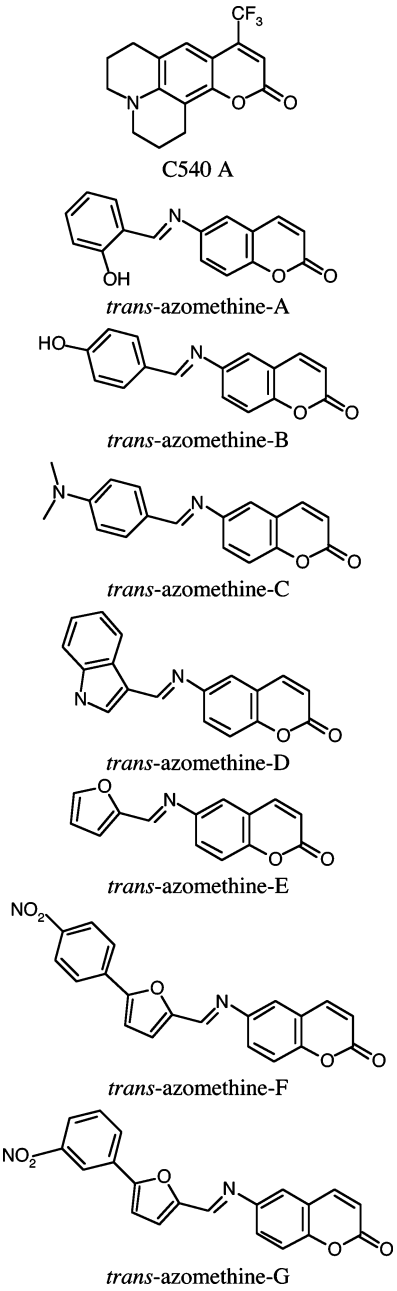

Figure 6. Sketch of C540 A and other studied azomethine dyes.

dipole moment is similar to the experimental value obtained by Moylan in chloroform.[39] A rotation of 40 ° induces a 9 nm bathoshift of the UV spectrum (a 0.12 eV decrease of the first transition energy), the influence on the second absorption band being even larger: 17 nm bathoshift or a 0.18 eV decrease of the second transition energy. The miss of such twisted geometries in our model can explain the difficulty to correctly describe the UV spectra of the amino coumarins.

Model Validation: Blind Test on an External Set. To confirm the validity of our models, external sets of dyes have been made up by several -diOH and -diMeO as well as combined substitution patterns (see Tables 4 and 5) for ethanol and methanol series. In particular, for the ethanol series (Table 4), we have added C540A (Figure 6) and larger systems such as *trans*-azomethine derivatives (Figure 6), as these compounds are widely used as laser dyes. It turns out that, in the MeOH series, the SLR-MAE are identical for $\lambda_{max}^{(1)}$ and $\lambda_{max}^{(2)}$: 5 nm or 0.06 eV, with maximum theory/experiment discrepancies limited to 12 nm or 0.14 eV for $\lambda_{max}^{(1)}$ and 9 nm or 0.17 eV for $\lambda_{max}^{(2)}$. This is in complete agreement with the SDR of eqs 5 and 6. On the other hand, for the EtOH series, the computed MAE are slightly larger (13 nm or 0.12 eV for $\lambda_{max}^{(1)}$ and 25 nm or 0.36 eV for $\lambda_{max}^{(2)}$; i.e., the accuracy is still satisfactory). As expected for amino coumarins, these figures confirm the good transferability of our procedure for λ_{max} determination in different solvents. Moreover, on the full set of the compounds treated in this study, only three cases with deviations exceeding 25 nm have been found: 7-Me,6-NO_2-coumarin and *trans*-azomethine-F and -G (Figure 6), molecules presenting a signifiant charge transfert involving the nitro group. For these molecules, it is well-known that conventional (TD)-DFT overshoots the charge transfer and underestimates the related transition energies.[40−42] Nevertheless our model is still on the trail for azomethine derivatives for which the MAE on the λ_{max} is of 23 nm, the same order of magnitude as our previous TD-DFT investigations of large systems derived from fluoro-anthraquinone dyes.[43] This definitively confirms the validity of eqs 3−6 for a quantitative evaluation of the electronic excitation energies of substitued pyranones.

Conclusions

We have established a procedure able to quantitatively evaluate the absorption spectrum of pyranone derivatives in ethanol and methanol. On the only basis of the agreement with experimental data, it was not obvious to choose among O3LYP, B3LYP, and PBE0. Nevertheless, using the auxochromic shift criterium, we favor PBE0 as this hybrid offers a nice agreement between theory and measurements. With PBE0, the theoretical auxochromic shifts are well-reproduced, and more essentially, the sign (batho/hypso) of the shift is almost always correctly predicted. For each solvent, calibration curves improve the accuracy of the λ_{max}. For about eigthy substitued pyranones, the required accuracy for the design of new molecules has been reached. Indeed, the mean average error is 9 nm (0.13 eV), in line with previous TD-DFT results obtained for anthraquinone and thioindigo dyes.[44,45] This high accuracy results in part from the selection of an extended basis set and from the explicit consideration of bulk solvent effects. It is our experience that such effects are essential to obtain a satisfying experiment/theory agreement as well as a sound predictive ability. We are currently adapting our methodology to step ahead to the fluorescence spectra calculation of pyranones.

Acknowledgment. J.P. acknowledges the FRIA (Belgian "Fonds pour la Formation à la Recherche dans l'Industrie et dans l'Agriculture") for his Ph.D. grant. D.J. and E.A.P. thank the Belgian National Fund for their Research Associate positions. The calculations have been performed on the Interuniversity Scientific Computing Facility (ISCF), installed at the Facultés Universitaires Notre-Dame de la Paix (Namur, Belgium), for which the authors gratefully acknowledge the financial support of the FNRS-FRFC and the "Loterie Nationale" for the Convention No. 2.4578.02 and of the FUNDP.

References and Notes

(1) Hirsh, J.; Dalen, J. E.; Anderson, D. R.; Poller, L.; Bussey, H.; Ansell, J.; Deykin, D. *Chest* **2001**, *119*, 8S.

(2) Christie, R. M. *Colour Chemistry*; Royal Society of Chemistry: Cambridge, UK, 2001.

(3) Zollinger, H. *Color Chemistry. Syntheses, Properties, and Applications of Organic Dyes and Pigments*; Wiley-VCH: Zürich, 2003.

(4) Novak, I.; Kovac, B. *J. Electron. Spectrosc. Relat. Phenom.* **2000**, *113*, 9.

(5) Kovac, B.; Novak, I. *Spectrochim. Acta A* **2002**, *58*, 1483.

(6) Kachkovski, O. D.; Tolmachev, O. I.; Kobryn, L. O.; Bilba, E. E.; Ganushchak, M. I. *Dyes Pigm.* **2004**, *63*, 203.
(7) Jacquemin, D.; Preat, J.; Wathelet, V.; André, J. M.; Perpète, E. A. *Chem. Phys. Lett.* **2005**, *405*, 429.
(8) Jamorski-Jödicke, C.; Lüthi, H. P. *J. Am. Chem. Soc.* **2002**, *125*, 252.
(9) Wilberg, K. B.; de Oliveria, A. E.; Trucks, G. *J. Phys. Chem. A* **2002**, *106*, 4192.
(10) Guillaumont, D.; Nakamura, S. *Dyes Pigm.* **2000**, *46*, 85.
(11) Preat, J.; Jacquemin, D.; Perpète, E. A. *Chem. Phys. Lett.* **2005**, *415*, 20.
(12) Cossi, M.; Barone, V. *J. Chem. Phys*. **2001**, *115*, 4708.
(13) Adamo, C.; Barone, V. *Chem. Phys. Lett.* **2000**, *330*, 152.
(14) Baerends, E. J.; Ricciardi, G.; Rosa, A.; van Gisbergen, S. J. A. *Coord. Chem. Rev.* **2002**, *230*, 5.
(15) Cave, J.; Burke, K.; Castner, E. W. *J. Phys. Chem. A* **2002**, *106*, 9294.
(16) Cave, J.; Castner, E. W. *J. Phys. Chem. A* **2002**, *106*, 12117.
(17) Frisch, M. J.; Trucks, G. W.; Schlegel, H. B.; Scuseria, G. E.; Robb, M. A.; Cheeseman, J. R.; Montgomery, J. A., Jr.; Vreven, T.; Kudin, K. N.; Burant, J. C.; Millam, J. M.; Iyengar, S. S.; Tomasi, J.; Barone, V.; Mennucci, B.; Cossi, M.; Scalmani, G.; Rega, N.; Petersson, G. A.; Nakatsuji, H.; Hada, M.; Ehara, M.; Toyota, K.; Fukuda, R.; Hasegawa, J.; Ishida, M.; Nakajima, T.; Honda, Y.; Kitao, O.; Nakai, H.; Klene, M.; Li, X.; Knox, J. E.; Hratchian, H. P.; Cross, J. B.; Bakken, V.; Adamo, C.; Jaramillo, J.; Gomperts, R.; Stratmann, R. E.; Yazyev, O.; Austin, A. J.; Cammi, R.; Pomelli, C.; Ochterski, J. W.; Ayala, P. Y.; Morokuma, K.; Voth, G. A.; Salvador, P.; Dannenberg, J. J.; Zakrzewski, V. G.; Dapprich, S.; Daniels, A. D.; Strain, M. C.; Farkas, O.; Malick, D. K.; Rabuck, A. D.; Raghavachari, K.; Foresman, J. B.; Ortiz, J. V.; Cui, Q.; Baboul, A. G.; Clifford, S.; Cioslowski, J.; Stefanov, B. B.; Liu, G.; Liashenko, A.; Piskorz, P.; Komaromi, I.; Martin, R. L.; Fox, D. J.; Keith, T.; Al-Laham, M. A.; Peng, C. Y.; Nanayakkara, A.; Challacombe, M.; Gill, P. M. W.; Johnson, B.; Chen, W.; Wong, M. W.; Gonzalez, C.; Pople, J. A. *Gaussian 03*, revision B.04; Gaussian, Inc.: Wallingford, CT, 2004.
(18) Runge, E.; Gross, E. K. U. *Phys. Rev. Lett.* **1984**, *52*, 997.
(19) Becke, A. D. *Phys. Rev. A* **1988**, *38*, 3098.
(20) Lee, C.; Yang, W.; Parr, R. G. *Phys. Rev. B* **1988**, *37*, 785.
(21) Perdew, J. P.; Burke, K.; Ernzerhof, M. *Phys. Rev. Lett.* **1997**, *78*, 1396.
(22) van Voohris, T.; Scuseria, G. E. *J. Chem. Phys.* **1998**, *109*, 400.
(23) Hoe, W. M.; Cohen, A. J.; Handy, N. C. *Chem. Phys. Lett.* **2001**, *341*, 319.
(24) Becke, A. D. *J. Chem. Phys.* **1993**, *98*, 5648.
(25) Ernzerhof, M.; Scuseria, G. E. *J. Chem. Phys.* **1999**, *110*, 5029.
(26) Adamo, C.; Barone, V. *J. Chem. Phys.* **1999**, *110*, 6158.
(27) Handy, N. C.; Cohen, A. J. *Mol. Phys.* **2001**, *99*, 403.
(28) Amovilli, C.; Barone, V.; Cammi, R.; Cancès, E.; Cossi, M.; Mennucci, B.; Pomelli, C. S.; Tomasi, J. *Adv. Quantum Chem.* **1998**, *32*, 227.
(29) Tomasi, J.; Mennucci, B.; Cammi, R. *Chem. Rev.* **2005**, *105*, 2999.
(30) Dagnelie, P. *Statistique Théorique et Appliquée*, Tome 1 & 2; De Boeck and Larcier: Bruxelles, 1998.
(31) Pollard, J. *A Handbook of Numerical and Statistical Techniques*; Cambridge University Press: Cambridge, UK, 1979.
(32) *Statgraphics Plus 5.1*; Manugistics Inc.: 2000.
(33) Masrani, K. V.; Rama, H. S.; Bafna, S. L. *J. Appl. Chem. Biotechnol.* **1974**, *24*, 311.
(34) Gonzalez, A. G.; Barroso, J. T.; Jorge, Z. D.; Rodriguez Luiz, F. *Rev. R. Acad. Cienc. Exactas, Fis. Nat. Madrid* **1981**, *75*, 811.
(35) Gnaguly, B. K.; Bagchi, P. *J. Org. Chem.* **1956**, *21*, 1415.
(36) Kalyanmay, S.; Bagchi, P. *J. Org. Chem.* **1959**, *24*, 316.
(37) *The Aldrich Handbook of Fine Chemicals and Laboratory Equipment*; Aldrich: Bornem, Belgium, 2003−2004.
(38) Burke, K.; Werschnik, J.; Gross, E. K. U. *J. Chem. Phys.* **2005**, *123*, 062206.
(39) Moylan, C. R. *J. Phys. Chem.* **1994**, *98*, 13513.
(40) Champagne, B.; Perpète, E. A.; Jacquemin, D.; A van Gisbergen, S. J.; Baerends, E. J.; Soubra-Ghaoui, C.; Robins, K. A.; Kirtman, B. *J. Phys. Chem. A* **2000**, *104*, 4755.
(41) Tozer, D. J. *J. Chem. Phys.* **2003**, *119*, 12697.
(42) Dreuw, A.; Head-Gordon, M. *J. Am. Chem. Soc*. **2004**, *126*, 4007.
(43) Preat, J.; Jacquemin, D.; Perpète, E. A. *Dyes Pigm.* (in press).
(44) Jacquemin, D.; Preat, J.; Charlot, M.; Wathelet, V.; André, J. M.; Perpète, E. A. *J. Chem. Phys.* **2004**, *121*, 1736.
(45) Jacquemin, D.; Preat, J.; Wathelet, V.; Fontaine, M.; Perpète, E. A. *J. Am. Chem. Soc*. **2006**, *128*, 2072.